Coated Colloids with Tailored Optical Properties

Verónica Salgueiriño-Maceira,[†] Frank Caruso,*[,‡] and Luis M. Liz-Marzán*[,†]

Departamento de Química Física, Universidade de Vigo, 36200, Vigo, Spain, and Department of Chemical and Biomolecular Engineering, The University of Melbourne, Victoria 3010, Australia

Received: February 5, 2003; In Final Form: July 24, 2003

Tailored optical properties have been imparted to polystyrene (PS) colloids of various sizes by the layer-by-layer (LbL) assembly of silica-coated gold ($Au@SiO_2$) or silica-coated silver ($Ag@SiO_2$) nanoparticles with different shell thicknesses and an electrostatically bridging polyelectrolyte, poly(diallyldimethylammonium chloride) (PDADMAC). The spectral position of the surface plasmon band of the composite colloid spheres is tailored through (i) the type of silica-coated nanoparticles used, (ii) the thickness of the silica shell, and (iii) the number of nanoparticle layers deposited. For thin silica shells (<10 nm), the number of nanoparticle layers deposited on the PS particles influences the plasmon band position due to electromagnetic coupling between neighboring metal nanoparticle cores. However, in the case of thick silica shells (>18 nm), nanoparticle core−core interparticle interactions are fully prevented and the plasmon band position is unaffected. Additionally, silica dissolution with HF leads to compact nanoparticulate metal layers on the PS spheres. The particles prepared are expected to find use as novel building blocks with unique optical properties for integration into advanced materials.

Introduction

Recent studies[1−4] have shown that the optical properties of metal nanoparticle assemblies are highly dependent on the separation between neighboring particles. Such an effect, which is in close agreement with calculations based on effective medium theories (in particular with Maxwell−Garnett equations), arises from particle dipole−dipole coupling. The practical consequence of the coupling is a red shift of the collective surface plasmon resonance, so that the color of the assembly varies from deep red to purple and blue as the particles are brought progressively closer to each other.

Several different approaches have been proposed to modulate the separation between particles so that they can be equally spaced over the entire nanostructured system. Brust et al.[1] made use of thioalkanes with different chain lengths, while Ung et al.[2,3] reported the controlled deposition of rigid, transparent silica shells, which allowed them to span a much broader range of interparticle distances (0.5−50 nm). The results of the latter studies clearly show that when the separation is long enough, the dipole−dipole coupling is fully suppressed, so that the plasmon band is located precisely at the same position as that of dilute dispersions of the same nanoparticles in a medium with a refractive index similar to that of silica.[2,3] Recently, Malikova et al.[4] used the intercalation of inert (polymer or clay) layers between successive metal nanoparticle layers to suppress the nanoparticle dipole−dipole interactions.

We have shown in a preliminary study[5] that a procedure similar to that used by Ung et al.[2,3] to assemble nanoparticle thin films on flat substrates can be equally applied to assemble silica-coated gold ($Au@SiO_2$) nanoparticles on the surface of polystyrene (PS) spheres. This strategy makes use of the layer-by-layer (LbL) technique[6] applied to colloids.[5,7−11] In that work,[5] we showed that the coupling between closely packed gold nanoparticles with thin silica shells (<5 nm) can also be observed for the nanoassemblies on spheres dispersed in solution. The interest in such assemblies lies in both their potential as novel colloids with tailored optical properties and their use as building blocks for the construction of more complex nanostructures, such as colloidal crystals.[12,13] These particles are significantly different from those coated with metallic shells, which have been reported for various colloid spheres[14−17] in that even though the metal is evenly distributed on the surface, the coated spheres can retain the plasmon resonance characteristic of small dispersed nanoparticles, exhibiting narrow and well-defined absorption bands in the visible range.[18] They are also different from other colloids decorated with metal nanoparticles,[13,19−22] as the interparticle separation between the $Au@SiO_2$ nanoparticles is precisely determined by the thickness of the silica shell. In a related study,[23] Cassagneau and Caruso reported the preparation of metallodielectric spheres with unique optical properties prepared by the LbL assembly of octa(3-aminopropyl)silsesquioxane (NSi8) stabilized silver nanoparticles (Ag@NSi8) and poly(styrenesulfonate), PSS, on silica and PS spheres. Additionally, upon calcination at 570 °C of the Ag@NSi8/PSS-coated PS spheres, hollow composite silica/silver spheres were obtained. In that work, the integrity of the nanoparticles (no coalescence) was preserved due to the presence of a thin silica spacer (1.5−2 nm), originating from the sintered NSi8 capping molecules.

In this paper, we present a detailed study on the preparation and characterization of PS particles coated with $Au@SiO_2$ nanoparticle layers via the LbL technique. PS spheres of different sizes have been used, on which gold nanoparticles (∼15 nm in diameter) coated with silica shells of various thicknesses (8−28 nm) have been deposited. The morphology of these nanostructured colloids was studied by means of transmission electron microscopy, and their optical properties were monitored

* To whom correspondence should be addressed. E-mail: lmarzan@uvigo.es (L.M.L.-M.).
[†] Universidade de Vigo.
[‡] The University of Melbourne.

10.1021/jp034302+ CCC: $25.00
Published on Web 09/11/2003

through UV−visible spectrophotometry. The results show that the optical behavior is very similar to that of thin films when scattering by the PS cores is taken into account, indicating that colloids with tailored optical properties can be prepared using this method. Results are also shown using $Ag@SiO_2$ nanoparticles (∼12 nm) coated with <2 and ∼10 nm thick silica shells, which agree with those for the gold nanoparticle systems, demonstrating that a wide spectral range can be spanned by using this procedure.

Experimental Section

Tetrachloroauric acid ($HAuCl_4$), silver perchlorate ($AgClO_4$), trisodium citrate, sodium borohydride ($NaBH_4$), (3-aminopropyl)trimethoxysilane (APS), sodium silicate solution ($Na_2O(SiO_2)_{3-5}$, 27 wt % SiO_2), tetraethyl orthosilicate (TEOS), poly(diallyldimethylammonium chloride) (PDADMAC), M_w < 200 000, and poly(sodium 4-styrenesulfonate) (PSS), M_w 70 000, were purchased from Aldrich. PSS was dialyzed against Milli-Q water (M_w cutoff 14 000). Negatively charged, sulfate-stabilized polystyrene (PS) spheres of diameter 270 ± 8, 420 ± 12, 640 ± 5, and 925 ± 10 nm were purchased from Microparticles GmbH, Berlin. Sodium chloride was obtained from Merck. The water used in all experiments was obtained from a Millipore Milli-Q purification system with a resistivity higher than 18.2 MΩ cm. $Au@SiO_2$ nanoparticles were synthesized as described elsewhere[24] and concentrated by centrifugation, which also allowed removal of the excess sodium silicate. The gold core diameter was 15 ± 2 nm in all cases. $Au@SiO_2$ samples with three different shell thicknesses were used in this study (total diameters 32 ± 5, 50 ± 5, and 70 ± 5 nm, corresponding to an average of 8, 18, and 28 nm thick silica shells, respectively). Ag@SiO2 nanoparticles were synthesized as described by Ung et al.[25] Briefly, colloidal silver was prepared by rapidly adding 1 mL of 0.01 M $AgClO_4$ to 99 mL of a vigorously stirred, ice-cold solution containing 1 mM $NaBH_4$ and 0.30 mM sodium citrate. The particles so prepared had a mean diameter of 12 nm. For the coating with silica, the surface was first activated with APS (150 μL, 1 mM) to generate siloxy groups receptive to silicate ion deposition. Then, the addition of sodium silicate (1.2 mL, 0.54 wt %, pH 10−11) leads to an initial nanometer thick mantle, and finally, controlled precipitation of residual silicate by the addition of ethanol (1:4 H_2O−EtOH) creates a homogeneous shell with an average thickness of 10 nm.

The final core−shell particles were prepared by using a well-established method for the assembly of nanoparticles on colloid spheres.[7−9] The method consists of depositing a precursor multilayer polyelectrolyte film (PDADMAC/PSS/PDADMAC) (PE_3) onto the PS spheres to generate a uniform surface charge and smooth coating, followed by the alternate deposition of $Au@SiO_2$ or $Ag@SiO_2$ nanoparticles and an oppositely charged bridging polyelectrolyte (PDADMAC). The polyelectrolyte-coated particles were prepared by taking 50 μL of a concentrated suspension of PS spheres (3.8 wt % solution), which was diluted with water to 1 mL, adding a 1 mL aliquot of PDADMAC (1 mg mL^{-1}, containing 0.5 M NaCl), waiting 15 min for PDADMAC adsorption, and then removing excess PDADMAC by three repeated centrifugation/wash cycles. The centrifugation speeds depended on the size of the PS spheres used: 19280*g*/10 min for 270 nm; 11900*g*/10 min for 420 nm; 3800*g*/10 min for 640 nm; 2460*g*/10 min for 925 nm. PSS (1 mg mL^{-1} containing 0.5 M NaCl) was then deposited onto the coated PS particles in a similar fashion and using the same conditions, followed by an additional layer of PDADMAC, which forms the outermost layer. The nanoparticle/polymer multilayers were formed via the electrostatic interactions between the silica surface (negatively charged under the assembly conditions) of the nanoparticles and PDADMAC, which acts as an electrostatic molecular glue between each $Au@SiO_2$ nanoparticle layer. Nanoparticle/PDADMAC multilayer coatings were deposited on the PS spheres as follows: 14 μL of the PE_3-coated PS particles (2.5 wt %) were dispersed in 0.5 mL of a 0.2 M NaCl solution, and then 0.5 mL of either a $Au@SiO_2$ or $Ag@SiO_2$ nanoparticle dispersion ([metal] = 0.015 M or 8.66×10^{13} nanoparticles mL^{-1}) was added. (This ensured that the final salt concentration of the solution from which nanoparticle adsorption proceeded was 0.1 M, facilitating a denser packing of the nanoparticles on the PS spheres.[7,10,11]) An adsorption time of 20 min was then allowed, and excess nanoparticles were removed by five repeated centrifugation (660*g*, 10 min)/wash cycles. PDADMAC (1 mg mL^{-1} solution containing 0.5 M NaCl, adsorption time of 20 min) was subsequently deposited and the excess removed from the supernatant after centrifugation (1200*g*, 10 min). Additional nanoparticle/PDADMAC multilayers were deposited as described above but with a lower centrifugation speed of 390*g* for the washing steps.

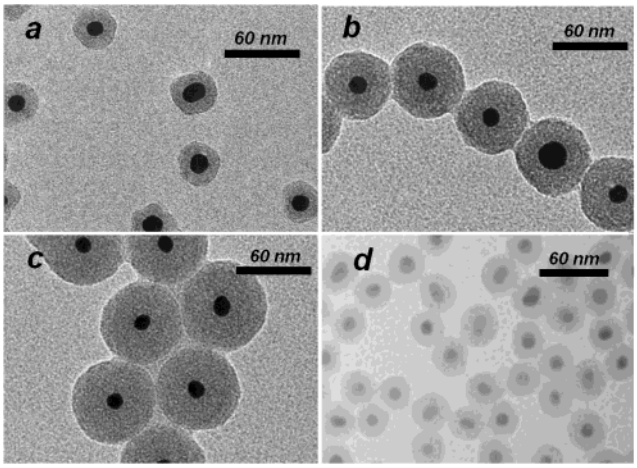

Figure 1. (a−c) TEM micrographs of the three different $Au@SiO_2$ nanoparticles used for LbL assembly onto PS spheres: (a) $Au@SiO_2$-30; (b) $Au@SiO_2$-50; (c) $Au@SiO_2$-70. All three images were obtained at the same magnification. (d) TEM micrograph of $Ag@SiO_2$ nanoparticles with 10 nm thick silica shells.

Silica removal after nanoparticle assembly on the PS spheres was accomplished by the addition of HF solution (1 wt %) to a dispersion of the core−shell particles. Silica dissolution (monitored spectroscopically) was complete after 2 h.

UV−vis absorption spectra of aqueous particle dispersions were recorded using an Agilent 8453 UV−visible spectrophotometer, either in standard transmission geometry or using a Labsphere RSA-HP-8453 integrating sphere. TEM measurements were performed with a JEOL JEM 1010 microscope operated at 100 kV or a Philips CM12 operated at 120 kV. Samples for TEM were prepared by sonicating the dispersions in water for 1 min and then depositing a drop onto a carbon-coated grid, which was allowed to dry in air.

Results and Discussion

One of the most important features to take into account for the interpretation of the results presented here is the quality of the $Au@SiO_2$ and $Ag@SiO_2$ nanoparticles used as building blocks. Both a narrow distribution in the core size and a high uniformity in the shell thickness are prerequisites to achieve reproducible optical properties of the composite colloids. Figure 1 shows representative TEM micrographs of the different core−

shell nanoparticles used, which illustrate that both the gold and silver cores are rather monodisperse and that the silica shells are highly uniform.

The impetus for assembling the silica-coated metal nanoparticles with different shell thicknesses onto submicron sized PS spheres is to modulate the optical properties of the final composite colloids. It has been shown that, on planar substrates,[2,3] control over the optical properties of Au@SiO_2 nanoparticulate films can be achieved when Au@SiO_2 nanoparticles are assembled layer-by-layer. In that case, control is based on the gradual screening of interparticle interactions as the shell thickness (and in turn the interparticle separation in close-packed nanoparticle films) increases. When the silica shell is thick enough (larger than ca. 15 nm), the plasmon band position does not depend on the shell thickness any longer, since dipole−dipole coupling between the gold cores is fully suppressed. Here, we have assembled the same gold nanoparticles coated with silica shells of varying thickness on PS spheres of different diameters, thus preparing a novel class of optically active core−shell colloids, and we have investigated the influence of curved substrates (i.e., colloid particles) of different size (and hence curvature) on the optical properties of Au@SiO_2 nanoparticle thin films. In addition, Ag@SiO_2 nanoparticles with different silica shell thicknesses have been assembled on PS core particles of 640 nm diameter.

Optimization of the deposition procedure was necessary to obtain dense, close-packed nanoparticle coatings on the surface of the template colloids. The conditions, described in the Experimental Section, have been found to be suitable for generating uniform and dense coatings of the nanoparticles for all three sizes. First, we report on the use of Au@SiO_2 nanoparticles. TEM images revealed the high and uniform quality of the coatings for composite particles of different composition (i.e., deposition stages) and for the Au@SiO_2 nanoparticles with different shell thicknesses (Figure 2). The low magnification TEM image in Figure 2a demonstrates the homogeneous coverage and close packing of the nanoparticles, which was achieved for all three Au@SiO_2 nanoparticle systems, regardless of the Au@SiO_2 nanoparticles used and the PS core size. In all cases, the nanoparticles form compact film assemblies on the surface of the PS spheres, so that the gold intercore distance is effectively determined by the silica shell thickness.

The extinction spectra of a series of coated colloids were measured, as shown in Figure 3. It is clear that, for the nanoparticles with thinner silica shells, the deposition of consecutive nanoparticle layers leads to a red-shift of the peak surface plasmon resonance due to interparticle interactions, in agreement with the results previously published[5] for even thinner silica shells. In contrast, for the nanoparticles with thicker silica shells, the peak plasmon position remains essentially unaltered with increasing Au@SiO_2 nanoparticle layer number. These results are consistent with those reported for similar assemblies prepared on planar substrates.[2] For the coatings comprised of Au@SiO_2 nanoparticles with thin silica shells (∼8 nm) (Figure 3a), the peak position of the surface plasmon band systematically red-shifts with the number of deposited layers, as a result of additional inter-nanoparticle interactions upon increasing the thickness of the Au@SiO_2 nanoparticle coatings. It has been shown, on planar supports for Au@SiO_2 nanoparticles with silica shells of thickness less than 15 nm, that only after at least 10 Au@SiO_2 nanoparticle layers are assembled the plasmon band becomes insensitive to the deposition of additional layers.

Another relevant issue is the dependence of the optical properties on the size of the substrate. To study this effect, we

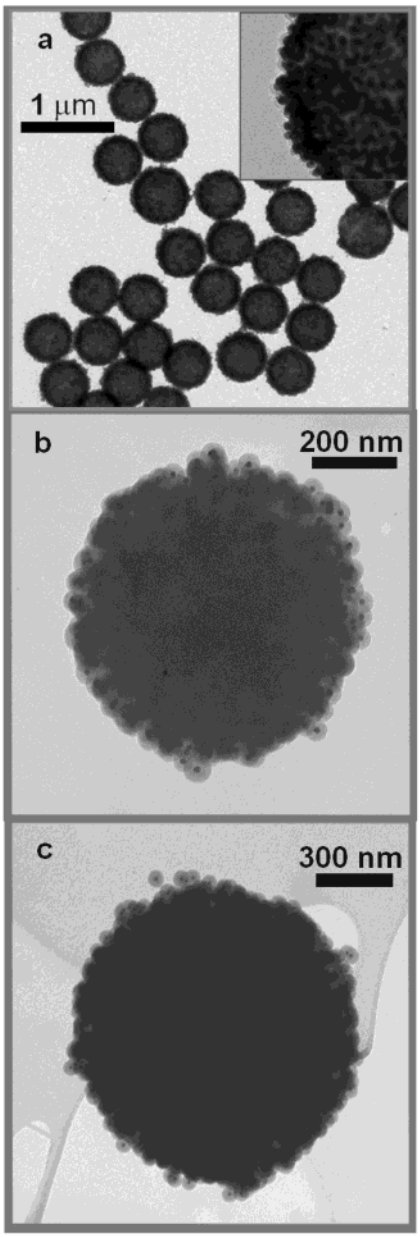

Figure 2. Various examples of PE_3-modified PS spheres coated with Au@SiO2 nanoparticle/PDADMAC multilayers: (a) a 640 PS sphere coated with two layers of 30 nm Au@SiO_2; (b) 640 PS spheres coated with one layer of 50 nm Au@SiO_2; (c) a 925 PS sphere coated with two layers of 70 nm Au@SiO_2. The inset in (a) is a higher magnification image, showing the dense packing of Au@SiO_2 nanoparticles on the PS sphere surface.

deposited the smaller Au@SiO_2 nanoparticles (30 nm) onto PS spheres of different diameters. The choice of the smaller nanoparticles for this experiment is based on the variation of the plasmon band position as a function of the number of layers deposited with this system. A summary of the results is shown in Figure 4. The first observation is that, for the same number of Au@SiO_2 nanoparticle layers, the plasmon band is consistently shifted toward higher wavelengths as the diameter of the PS core increases. However, the slope is similar for the four samples, which indicates that the different behavior originates from the larger scattering of light as the PS core size is increased. Additionally, the long tails in the spectra (Figure 3) indicate the presence of light scattering in the systems.

The influence of light scattering was confirmed by using a different setup to measure transmission spectra. In this case,

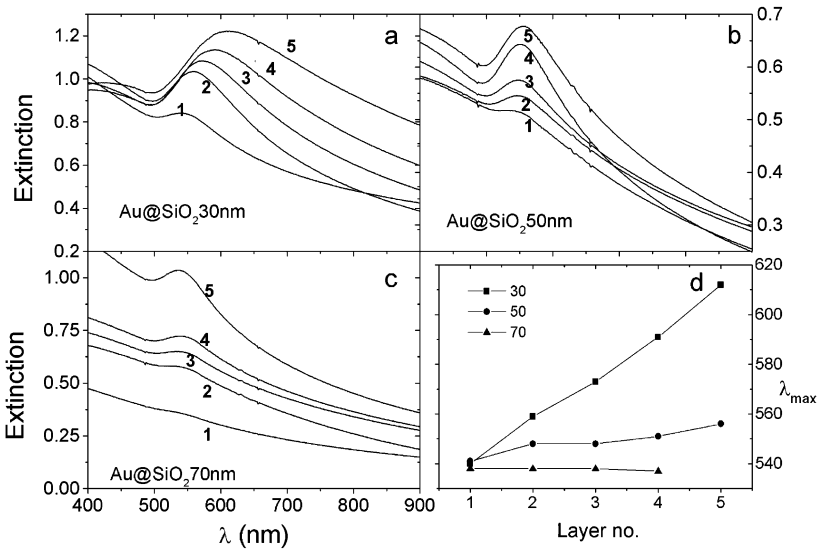

Figure 3. (a−c) Extinction spectra of $Au@SiO_2$ nanoparticle/PDADMAC multilayer-coated PS spheres with different multilayer shell thicknesses dispersed in aqueous solution. The number of deposition cycles and the outer diameters of the $Au@SiO_2$ nanoparticles are indicated. (d) Maximum position of the surface plasmon band for 640 PS spheres coated with a different number of layers of $Au@SiO_2$ nanoparticles of various diameters, as indicated.

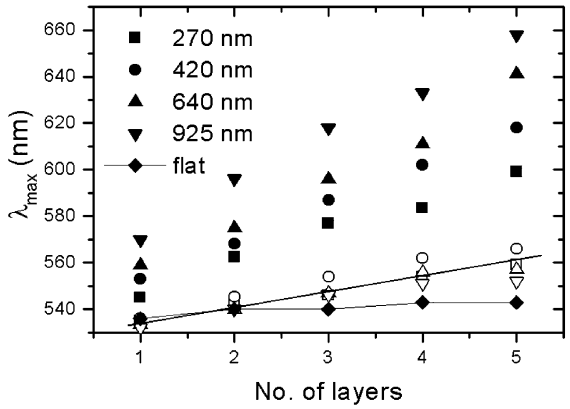

Figure 4. Maximum position of the plasmon band for PS spheres of various sizes coated with a different number of layers of $Au@SiO_2$ nanoparticles (core diameter = 20 nm, shell thickness = 10 nm). Full symbols refer to standard absorbance measurements; open symbols refer to the use of an integrating sphere.

we made use of an integrating sphere (IS), so that the scattering contribution to the signal is strongly reduced. Such a method for minimizing scattering from quantum dot assemblies was recently reported by Döllefeld et al.[26] in a study of quantum dot interparticle interactions. By means of the IS measurements, we observe only a red-shift in the plasmon band position when the thinly coated $Au@SiO_2$ nanoparticles (30 nm total diameter) are assembled. An example is given in Figure 4, where the plasmon band peak position is plotted as a function of the number of layers for 20 nm gold nanoparticles coated with 10 nm thick silica shells assembled onto PS spheres of different size. In this case, gold−gold interparticle interactions are slightly stronger than those shown in Figure 3, due to the larger gold core size used in these experiments (20 vs 15 nm). For comparison, the peak positions of the plasmon bands of planar assemblies (measured with the standard absorbance setup) of the same coated nanoparticles have also been plotted in the same figure, which are very close to those measured using the IS setup.

A similar study was also performed for PS spheres coated with $Ag@SiO_2$ nanoparticles. In this case only two samples were used: one with a very thin (<2 nm) silica shell deposited on

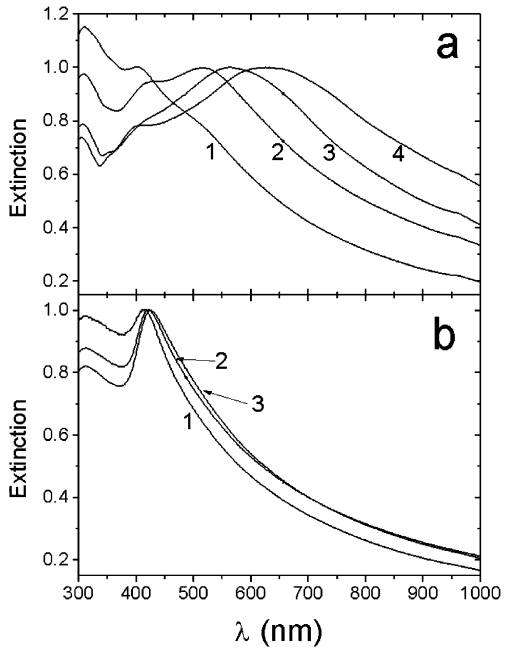

Figure 5. Normalized extinction spectra of $Ag@SiO_2$ nanoparticle/PDADMAC multilayer-coated PS spheres with different multilayer shell thicknesses dispersed in aqueous solution. In (a), the silica shell thickness on the $Ag@SiO_2$ nanoparticles is <2 nm, and it is ∼10 nm for the data shown in (b). The numbers of deposition cycles are indicated.

the silver cores from aqueous sodium silicate and another with a shell thickness of ca. 10 nm deposited by controlled precipitation of residual silicate through ethanol addition (Figure 5). The deposition of thicker shells on Ag cores is complicated by the aerial oxidation of the core driven by the ammonia used as a catalyst for silica growth.[25] LbL assembly of the $Ag@SiO_2$ nanoparticles on 640 nm PS spheres could be performed by using the same conditions optimized for $Au@SiO_2$, since the nature of the silica surface is virtually identical. As expected, the trends in the optical properties measured are similar to those reported above for gold. Assembly of silver cores with very thin shells leads to a pronounced red-shift of the plasmon band due to inter-nanoparticle interactions, while when using silver

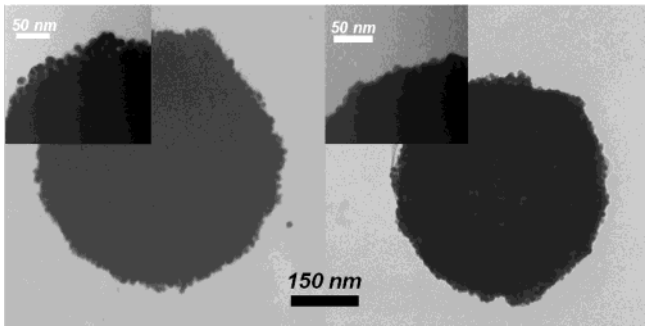

Figure 6. TEM micrographs of 420 nm PS spheres coated with five layers of 30 nm Au@SiO_2 nanoparticles (left) and the same sample after HF treatment (right). The insets show higher magnifications of the corresponding surface, where the presence of silica shells in the sample before HF treatment can be seen but not in the HF-treated sample.

nanoparticles coated with 10 nm shells, the plasmon band peak position shifts only very slightly (from 416 to 418 nm) through several deposition steps.

This shows not only that the optical effects are indeed due to interparticle interactions when the silica shells are thin enough but also that this assembly procedure can be utilized to deposit a variety of silica coated nanoparticles and impart the properties of the individual nanoparticles to the composite, larger colloids.

In a previous paper,[5] we demonstrated that the PS core of the composite colloid particles described here can be decomposed through calcination, so that hollow metallo-dielectric spheres are obtained, which is an example of the potential of this system for the preparation of compositionally diverse particles. A different modification that can be performed to this system is via the dissolution of the silica shells, using HF. In this way, conducting colloid spheres can potentially be obtained, since direct contact between the Au nanoparticles may be achieved upon removal of the shells encapsulating each gold nanoparticle. Experiments were conducted where 1 wt % HF solution was added to a dispersion of 420 nm PS spheres coated with 5 layers of 30 nm Au@SiO_2 nanoparticles. TEM micrographs of the starting and the final composite spheres are shown in Figure 6. It is clear that upon dissolution there is a reduction in total diameter of ca. 100 nm, which is consistent with the removal of the silica shells present. The absence of silica after dissolution was confirmed by EDS, where no Si peak was detected.

The effect of silica dissolution on the optical properties of the dispersion was also studied. A further red shift (622 to 649 nm) was observed with respect to the HF-untreated sample. However, the spectrum does not correspond to what would be expected for continuous gold nanoshells of similar dimensions.[14] This is probably due to the presence of the polyelectrolyte layers between metal nanoparticle layers, which can screen the interparticle interactions, as was recently shown for LbL films made of "flat" gold nanoparticles.[4] Such polyelectrolyte can be removed by heating the samples at elevated temperature, as previously reported.[5]

Conclusions

We have demonstrated the assembly of silica-coated gold and silver nanoparticles with various shell thicknesses onto latex spheres of various diameters. The optical properties of the final, composite particles are dependent on the morphology of the Au- and Ag@SiO_2 building units, the number of nanoparticle layers deposited, and the size of the substrates. It is important to take into account the scattering contribution due to the large particle size, which can affect the optical properties of the colloidal dispersions. This, however, can be suppressed through proper choice of the solvent. It has also been shown that the silica shells encapsulating the gold nanoparticles can be removed after their assembly, so that the gold nanoparticles are in mutual contact.

Acknowledgment. L.M.L.-M. acknowledges financial support from the Spanish Xunta de Galicia (Project No. PGIDT01PXI30106PR) and Ministerio de Ciencia y Tecnología (Project No. BQU2001-3799). F.C acknowledges financial support from the BMBF and the Australian Research Council under the Federation Fellowship and Discovery Project schemes. The authors are indebted to J. B. Rodríguez-González (CACTI, Universidade de Vigo) and U. Bloeck (Hahn-Meitner-Institute) for assistance with TEM measurements.

References and Notes

(1) Brust, M.; Bethell, D.; Kiely, C. J.; Schiffrin, D. J. *Langmuir* **1998**, *14*, 5425.
(2) Ung, T.; Liz-Marzán, L. M.; Mulvaney, P. *J. Phys. Chem. B* **2001**, *105*, 3441.
(3) Ung, T.; Liz-Marzán, L. M.; Mulvaney, P. *Colloid Surf., A* **2002**, *202*, 119.
(4) Malikova, N.; Pastoriza-Santos, I.; Schierhorn, M.; Kotov, N. A.; Liz-Marzán, L. M. *Langmuir* **2002**, *18*, 3694.
(5) Caruso, F.; Spasova, M.; Salgueiriño-Maceira, V.; Liz-Marzán, L. M. *Adv. Mater.* **2001**, *13*, 1090.
(6) Decher, G.; Hong, J. D. *Ber. Bunsen-Ges. Phys. Chem.* **1991**, *95*, 1430.
(7) (a) Caruso, F.; Caruso, R. A.; Möhwald, H. *Science* **1998**, *282*, 1111. (b) Caruso, F.; Caruso, R. A.; Möhwald, H. *Chem. Mater.* **1999**, *11*, 3309.
(8) Caruso, F. *Chem.—Eur. J.* **2000**, *6*, 413.
(9) Caruso, F. *Adv. Mater.* **2001**, *13*, 1.
(10) Caruso, F.; Lichtenfeld, H.; Möhwald, H.; Giersig, M. *J. Am. Chem. Soc.* **1998**, *120*, 8523.
(11) Caruso, F.; Möhwald, H. *Langmuir* **1999**, *15*, 8276.
(12) (a) Velev, O. D.; Tessier, P. M.; Lenhoff, A. M.; Kaler, E. W. *Nature* **1999**, *401*, 548. (b) Jiang, P.; Cizeron, J.; Bertone, J. F.; Colvin, V. L. *J. Am. Chem. Soc.* **1999**, *121*, 7957.
(13) Liang, Z.; Susha, A. S.; Caruso, F. *Adv. Mater.* **2002**, *14*, 1160.
(14) Oldenburg, S. J.; Averitt, R. D.; Westcott, S. L.; Halas, N. J. *Chem. Phys. Lett.* **1998**, *288*, 243.
(15) Jackson, J. B.; Halas, N. J. *J. Phys. Chem. B* **2001**, *105*, 2743.
(16) Graf, C.; van Blaaderen, A. *Langmuir* **2002**, *18*, 524.
(17) Schierhorn, M.; Liz-Marzán, L. M. *Nano Lett.* **2002**, *2*, 13.
(18) Kreibig, U.; Vollmer, M. *Optical Properties of Metal Clusters*; Springer: Berlin, 1995.
(19) (a) Arul Dhas, N.; Zaban, A.; Gedanken, A. *Chem. Mater.* **1999**, *11*, 806. (b) Zhong, Z.; Mastai, Y.; Koltypin, Y.; Zhao, Y.; Gedanken, A. *Chem. Mater.* **1999**, *11*, 2350. (c) Ramesh, S.; Cohen, Y.; Prosorov, R.; Shafi, K. V. P. M.; Aurbach, D.; Gedanken, A. *J. Phys. Chem. B* **1998**, *102*, 10234.
(20) Dokoutchaev, A.; James, J. T.; Koene, S. C.; Pathak, S.; Prakash, G. K. S.; Thompson, M. E. *Chem. Mater.* **1999**, *11*, 2389.
(21) Kobayashi, Y.; Salgueiriño-Maceira, V.; Liz-Marzán, L. M. *Chem. Mater.* **2001**, *13*, 1630.
(22) Gittins, D. I.; Susha, A. S.; Schoeler, B.; Caruso, F. *Adv. Mater.* **2002**, *14*, 508.
(23) Cassagneau, T.; Caruso, F. *Adv. Mater.* **2002**, *14*, 732.
(24) Liz-Marzán, L. M.; Giersig, M.; Mulvaney, P. *Langmuir* **1996**, *12*, 4329.
(25) Ung, T.; Liz-Marzán, L. M.; Mulvaney, P. *Langmuir* **1998**, *14*, 3740.
(26) Döllefeld, H.; Weller, H.; Eychmüller, A. *J. Phys. Chem. B* **2002**, *106*, 5604.